Chemistry and Physics of Lipids 163 (2010) 561–568

Contents lists available at ScienceDirect

Chemistry and Physics of Lipids

journal homepage: www.elsevier.com/locate/chemphyslip

Concentration and pH-dependent aggregation behavior of an L-histidine based amphiphile in aqueous solution

Arjun Ghosh, Saurabh Shrivastava, Joykrishna Dey*

Department of Chemistry, Indian Institute of Technology, Kharagpur 721302, India

ARTICLE INFO

Article history:
Received 22 December 2009
Received in revised form 9 March 2010
Accepted 6 April 2010
Available online 14 April 2010

Keywords:
Surface activity
Vesicles
Nanotubes
Fluorescence
Electron microscopy

ABSTRACT

The surface activity and self-assembly behavior of zwitterionic amphiphile N-(2-hydroxydodecyl)-L-histidine (C_{12}HHis) were studied in phosphate buffers of pH 2 and 13 using surface tension and fluorescence probe techniques, respectively. Transmission electron microscopic images of the aggregates have revealed existence of nano-size vesicles in dilute solutions of both acidic and basic pH. In basic medium, the vesicles are converted to tubular aggregates upon increase of surfactant concentration. The nanotubes undergo phase transition to form elongated or small rod-like micelles at a much higher concentration of the amphiphile. The vesicles and nanotubes were found to become more stable upon addition of 10 mol% of cholesterol.

1. Introduction

Histidine is considered to be an essential amino acid in human infants and becomes a non-essential amino acid for the adult. Histidine has the functions to treat tummy and hookworm. Presence of histidine in protein cause buffering and is a common coordinating ligand in metalloproteins and is a part of catalytic sites in certain enzymes (Bertini and Scozzafava, 1981; Casolaro et al., 2002; Kowalik-Jankowska et al., 1999; Bonomo et al., 1996). Bhattacharya and coworkers have demonstrated formation of helical structures in aqueous solution of N-acyl-L-histidine surfactants (Ragunath and Bhattacharya, 1995). Histidine is believed to be a membrane binding residue. Mono-histidylated cationic amphiphiles have been reported to have remarkable gene transfection properties via the endosome-disrupting characteristics of the histidine functionalities (Kumar et al., 2003). On the other hand, comicelles of N-acyl-L-histidine and various cationic surfactants have been found to be very effective in stereo-selective micelle-catalyzed deacylation of long-chain amino acid esters (Ohkubo et al., 1981). Antioxidant activity toward lipid peroxidation and excellent emulsifying activity of N-acyl-L-histidine have also been reported (Murase et al., 1993). In fact, histidine-derived amphiphiles behave as an unusual surfactant because the hydrophilic part contains a carboxylate group and an imidazole side-chain, offering the molecule pH responsive properties (Smith and Barden, 1975; Ihara et al., 1981). Smith et al. have reported an unusual effect of salt concentration on the critical micelle concentration (CMC) of the N-acyl-L-histidine surfactants (Smith and Barden, 1975). Because of potential uses of N-acyl-L-histidine it seemed important to us to look at the type of self-assemblies that could be formed by this class of amphiphiles in water.

In the present work, self-assembly properties of N-(2-hydroxydodecyl)-L-histidine, C_{12}HHis (see Scheme 1 for structure), was studied. Recently we have investigated the self-assembly properties of N-(2-hydroxydodecyl)-L-valine (C_{12}HVal) (Ghosh and Dey, 2008a), and N-(2-hydroxydodecyl)-L-alanine (C_{12}HAla) (Ghosh and Dey, 2008b) amphiphiles in aqueous medium. The former amphiphile has been found to form branching tubular structures where the latter was observed to form vesicles and twisted ribbon-like microstructures. Because of this striking difference in self-organization behavior, it seemed important to us to look at the type of self-assemblies that could be formed by the L-histidine-derived surfactant. The surface activity and aggregation behavior of the amphiphile were studied using surface tension, fluorescence, and dynamic light scattering techniques. Microstructure of the self-assemblies has been examined by transmission electron microscopy. Stability of the aggregates in the presence of salt and cholesterol, and with temperature change has also been investigated.

2. Materials and methods

2.1. Materials

Cholesterol, N-phenyl-1-naphthylaniline (NPN) and 1,6-diphenyl-1,3,5-hexatriene (DPH), and 1,2-epoxydodecane were

* Corresponding author. Tel.: +91 3222 283308; fax: +91 3222 255303.
E-mail address: joydey@chem.iitkgp.ernet.in (J. Dey).

0009-3084/$ – see front matter © 2010 Elsevier Ireland Ltd. All rights reserved.
doi:10.1016/j.chemphyslip.2010.04.003

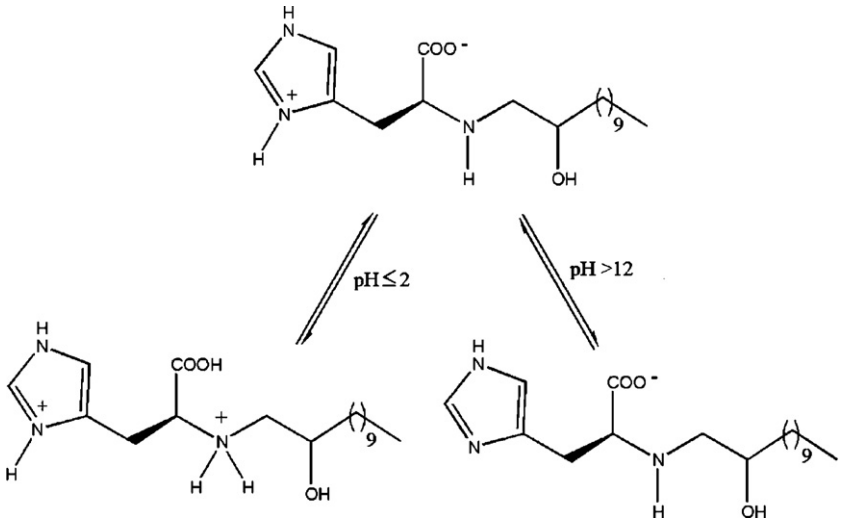

Scheme 1. Prototropic equilibria in aqueous solution of C_{12}HHis.

obtained from Aldrich (Milwaukee, WI, USA). The fluorescent probes NPN and DPH were purified by repeated recrystallization from ethanol-acetone mixture. Cholesterol, 1,2-epoxy-dodecane, and L-histidine (SRL, Mumbai) were used without further purification. All solvents used were obtained locally and were distilled and dried whenever required. Analytical grade disodium hydrogen phosphate, sodium hydroxide and hydrochloric acid were procured locally and were used directly from the bottle. The amphiphile *N*-(2-hydroxydodecyl)-L-histidine was prepared according to the procedure described elsewhere (Hidaka et al., 1984; Watanabe et al., 1988) and was purified by recrystallization from ethanol or ethanol-water mixture. The chemical structure of the amphiphile was identified and checked for purity by usual methods (IR, ^{1}H NMR, TLC). The ^{1}H NMR spectrum of the amphiphile has been shown in Fig. 1.

2.2. Methods

The ^{1}H and ^{13}C NMR spectra were recorded on a Bruker AVANCE 400 MHz instrument. Surface tension measurements were carried out with a surface tensiometer (model 3S, GBX, France) using Du Nuöy ring detachment method. A Thermo Orion (model 710 A+) pH meter that uses a combined glass electrode was used for all pH measurements. All measurements were carried out at room temperature (~303 K) unless otherwise mentioned.

All the solutions containing different concentrations of amphiphiles were prepared in pH 13 phosphate buffer made using double distilled water and were stored in closed glass bottles. For solutions containing cholesterol were prepared by first mixing aliquots from C_{12}HHis and cholesterol stock solutions in methanol in volumetric flasks. The solvent was then evaporated by purging dry nitrogen and finally dried in vacuum desiccators for 5–6 h. The solid mixture was diluted with required volume of 20 mM phosphate buffer (pH 2 or 13.0) and sonicated for 5 min.

Steady-state fluorescence spectra of NPN and DPH probes were measured on a PerkinElmer LS-55 luminescence spectrometer equipped with filter polarizers that uses the L-format configuration. Since NPN and DPH are poorly soluble in water, a stock solution (1.0 mM) of the probe in methanol was prepared. The final concentration of the probe was adjusted to 1.0 μM in the case of DPH and 10 μM in the case of NPN by addition of an appropriate amount of the stock solution. All fluorescence measurements started 2–3 h after sample preparation. Solutions containing NPN were excited at 360 nm. For steady-state fluorescence anisotropy measurements, DPH was excited at 350 nm and the fluorescence intensity was measured at 450 nm. A 430 nm cutoff filter was placed in the emission beam to reduce the effect of scattered light, if any. The excitation and emission slit widths were 2.5 and 5 nm, respectively. The software supplied by the manufacturer automatically determined the correction factor and anisotropy value. In all cases, the anisotropy values were averaged over an integration time of 10 s and maximum number of five measurements for each sample. The temperature (303 ± 0.1 K) of the water-jacketed cell holder was controlled by use of a JEO TECH RW-0525G circulating bath.

Time-resolved fluorescence measurements were performed on a time-correlated single-photon counting method. Fluorescence lifetimes were determined from time-resolved intensity decay by the method of time-correlated single-photon counting that uses a picosecond diode laser at 370 nm (IBH, UK, nanoLED-07) as light source. The typical response time of this laser system was 70 ps. The decays were analyzed using IBH DAS-6 decay analysis software. For all the lifetime measurements the fluorescence decay curves were analyzed by biexponential or triexponential iterative fitting program provided by IBH.

The dynamic light scattering (DLS) measurements were performed with a Zetasizer Nano ZS (Malvern Instrument Lab, Malvem, UK) optical system equipped with an He–Ne laser operated at 4 mW at λ_o = 632.8 nm, and a digital correlator. The solution was filtered directly into the scattering cell through a Millipore Millex syringe filter (Triton free, 0.45 μm). Before measurement, the scattering cell was rinsed several times with the filtered solution. The data acquisition started after 10 min and each experiment was repeated at least two times. Apparent diffusion coefficients (D_{app}) were calculated by first-order cumulant analysis of an autocorrelation function of scattered light intensity fluctuations. Effective hydrodynamic diameter (d_H) were calculated from diffusion coefficients using the Stokes–Einstein equation:

$$D_{app} = \frac{k_B T}{3\pi\eta d_H} \quad (1)$$

where k_B, η, and T are Boltzmann constant, viscosity of the solvent and absolute temperature, respectively.

The specimens for TEM measurements were prepared by placing 5 μL of the surfactant solution (pH 13) on a 400 mesh carbon-coated copper grid and allowed to adsorb for a minute. The excess liquid was then wicked off with a filter paper, air-dried, and negatively stained with freshly prepared 0.75% aqueous sodium phosphotungstate (pH 13). The specimens were dried overnight

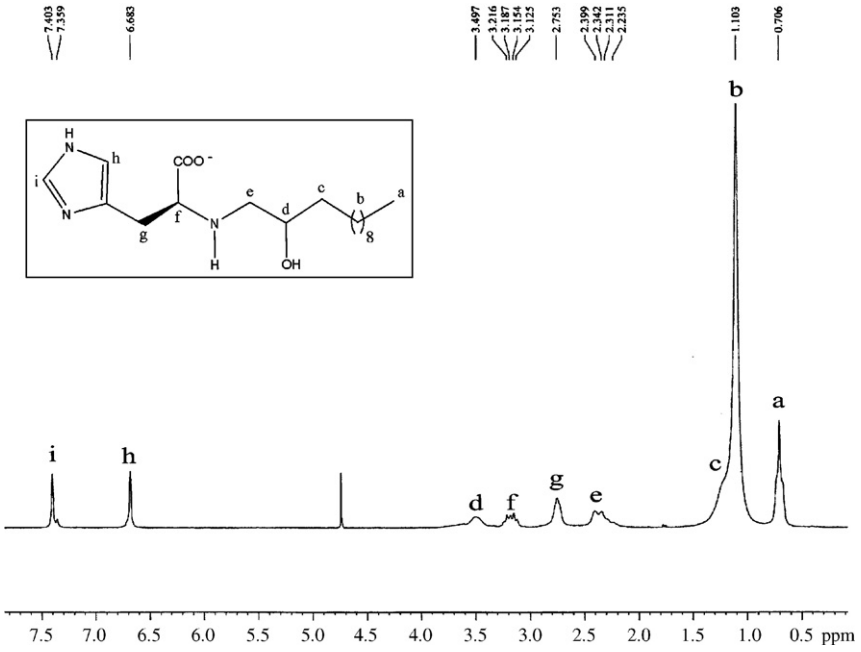

Fig. 1. ^{1}H NMR spectrum of C_{12}HHis in D_2O/NaOD solvent.

in desiccators before measurement with an electron microscope (JEOL-JEM 2100, Japan) operating at 200 kV.

3. Result and discussion

The amphiphile C_{12}HHis has ionizable imidazole ring apart from COOH group. Thus, depending upon the solution pH C_{12}HHis can exist in the form of anion, monocation, dication, and zwitterions or as a mixture of two. The prototropic species were found to be poorly soluble in all pHs, except at 12 < pH < 3. Therefore, all studies were performed in solutions of pH 2 and 13. At pH > 12, the dominant form is expected to be anionic, but at pH < 3, only dication specie exists in solution (Scheme 1). However, it should be noted that the dication has also limited solubility (<0.3 mM) in water at 303 K.

3.1. Critical aggregation concentration

Surface tension (γ) measurements were performed to determine critical aggregation concentration (CAC) of the surfactant. The plots of γ versus log[C_{12}HHis] for the aqueous buffer solutions (pH 2 and 13) of the amphiphile are presented in Fig. 2. Both plots exhibit two breaks as indicated by the upward arrows. This might be either due to phase change of the surfactant monolayer at the air/water interface or stepwise aggregation of the surfactant in solution. Phase transitions of Langmuir monolayers of lipids at the air/water interface as a result of even small changes in monolayer density or physical variables, such as temperature, pH, ionic strength, and composition of the subphase have been reported in the literature (Wang et al., 2005; Velázquez et al., 2005). However, in the present case, based on fluorescence probe study as described below, the double breaks in the surface tension plot can be attributed to stepwise aggregation of the amphiphile in solution. Thus the concentrations corresponding to the first and second break can be considered as CAC_1 and CAC_2, respectively. The CAC values obtained from the break points of the surface tension plots are listed in Table 1. The CAC values of both anionic and cationic forms are very low as compared to N^{α}-dedecanoyl-L-histidine (1.0 mM) amphiphile (Smith and Barden, 1975) The γ_{CAC2} values suggest that the anionic form is more surface active than the cationic specie. The

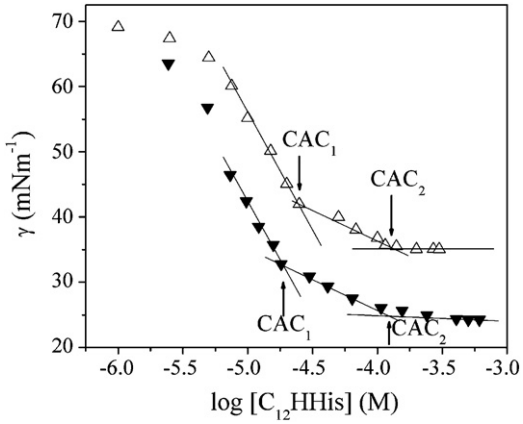

Fig. 2. Plots of surface tension (γ) versus log[C_{12}HHis] in 20 mM phosphate buffer (△) pH 2.0, (▼) pH 13.0 at 303 K.

surface area per surfactant headgroup, A_{min}, was calculated from the slope (corresponding to the part showing steepest decrease in γ) of the plots using Gibbs adsorption equation (Rosen, 2004):

$$\Gamma_{max} = -\frac{1}{nRT}\frac{d\gamma}{d\ln C} \quad (2)$$

Table 1
Critical aggregation concentrations (CACs), surface tension at CAC, surface excess concentration (Γ_{max}), minimum area per head group (A_{min}), packing parameter (P) of C_{12}HHis, and hydrodynamic diameters (d_H) of the vesicles in solutions of different pH at 303 K.

Properties	pH 13	pH 2
CAC_1 (mM)	0.02 (0.03)[a]	0.025 (0.03)[a]
CAC_2 (mM)	0.14 (0.13)[a]	0.14 (0.08)[a]
γ_{CAC2} (mN m^{-1})	24.3	34.9
$\Gamma_{max} \times 10^6$ (mol m^{-2})	4.44	3.25
A_{min} (nm^2 molecule^{-1})	0.37	0.51
P	0.72	0.52
d_H (nm)	70 (87)[b]	35 (55)[b]

[a] Data within the parentheses were obtained from fluorescence titration.
[b] Data within the parentheses were obtained in the presence of 10 mol% Chol.

where Γ_{max} (molecules/m^2) is the maximum surface excess concentration, n is the number of molecular species involved, and C is the concentration of surfactant. For the anionic and cationic forms of C_{12}HHis n-value was assumed to be equal to 1.0 and 2.0, respectively since the surface tension measurements were carried out in the presence of salt (20 mM) of relatively high concentration. Gibbs adsorption isotherm allows one to determine the minimum surface area (A_{min}) occupied by a surfactant head group at the air-water interface from the following equation:

$$A_{min} = \frac{1}{N_A \Gamma_{max}} \quad (3)$$

where N_A is Avogadro's number. The corresponding Γ_{max} and A_{min} values of the anionic and cationic forms of the amphiphile have been collected in Table 1. It is observed that the A_{min} values are very small suggesting close packing of the hydrocarbon chains. The A_{min} values are close to those of other carboxylate surfactants (0.45 nm^2) reported in the literature (Huang et al., 1999). In fact, it has been reported that in the case of histidine-derived amphiphiles, the imidazole ring functions as the polar head group with the NH directed toward the water surface resulting in a more condensed packing of the histidine amphiphiles (Smith and Barden, 1975; Abel et al., 2000) in which the imidazole rings are parallel to each other. The condensed packing in the case of C_{12}HHis is manifested in the higher value of packing parameter P (Table 1) calculated from Eq. (4) (Israelachvili, 1985):

$$P = \frac{v}{A_{min} l_c} \quad (4)$$

where v (0.372 nm^3) (Ghosh and Dey, 2008a) and l_c (1.40 nm) (Ghosh and Dey, 2008a) are the volume and length of the hydrocarbon chain. The large value of P (>0.5) indicates formation of bilayer aggregates at concentrations above CAC_1 of both anionic and cationic forms of the C_{12}HHis amphiphile.

3.2. Fluorescence probe studies

Morphological changes of surfactant aggregates often involve change in the chain packing and hence in their microenvironments. Fluorescent probes, such as NPN and DPH have been used extensively to study microenvironments of micellar aggregates (Félix and Goñi, 2000; Saitoh et al., 2007; Nemkovich et al., 1997). The emission maximum of NPN exhibits a large blue shift accompanied by a huge enhancement of emission intensity relative to that in water upon its incorporation into the hydrophobic environments of micelles (Nayak et al., 2006; Roy et al., 2006). On the other hand, steady-state fluorescence anisotropy (r) of DPH probe can be used to distinguish micelles from bilayer aggregates. Normally micelles of ionic surfactants have very low r-value (~0.05) and vesicles have r-value usually greater than 0.14 (Shinitzky, 1984; Zana et al., 1997; Roy et al., 2005). The self-assembly formation by C_{12}HHis was, therefore, studied using both NPN and DPH probes. The plot of relative fluorescence intensity (I/I_o) of NPN probe at pH 13 versus [C_{12}HHis] is shown in Fig. 3. The plot exhibits two inflections, one at a concentration around CAC_1 and the other at around CAC_2. This supports the surface tension data and thus confirms stepwise aggregation of C_{12}HHis in aqueous medium.

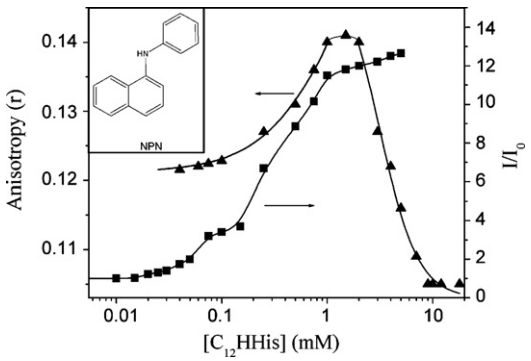

Fig. 3. Plots of relative fluorescence intensity (I/I_o) of NPN (■), and fluorescence anisotropy (r) of DPH (▲) probes versus [C_{12}HHis] in 20 mM phosphate buffer, pH 13.0 at 303 K; inset: chemical structure of NPN.

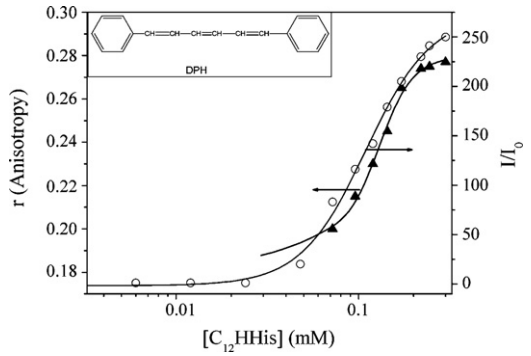

Fig. 4. Plots of relative fluorescence intensity, I/I_o (○) and fluorescence anisotropy, r (▲) of DPH versus [C_{12}HHis] in 20 mM phosphate buffer, pH 2.0 at 303 K; inset: chemical structure of DPH.

In order to study the concentration-dependent phase change, the fluorescence anisotropy of DPH probe was also measured at different [C_{12}HHis]. As shown in Fig. 3, the r-value above CAC_1 is quite high and can be associated with bilayer aggregates. With the rise in concentration the r-value increased following a sigmoid function reaching maximum at about 1.5 mM. This small rise of r-value might be due to growth of the bilayer aggregates. Similar feature can also be observed with the plot (Fig. 4) for surfactant solutions at pH 2. Fig. 4 also depicts plot of I/I_o of DPH probe versus [C_{12}HHis] in pH 2 solution. A huge rise in the fluorescence intensity of DPH probe is observed in presence of the cationic form which suggests very high solubility of the probe molecules in the aggregates formed in solution. However, unlike in pH 13 solution, the

Table 2
Steady-state fluorescence anisotropy (r), time-resolved fluorescence data, and microviscosity (η_m) of DPH probe in phosphate buffer solutions (pH 2 and 13) of different [C_{12}HHis] at 303 K.

pH	[C_{12}HHis] (mM)	τ_f (ns)	Amplitude (a)	χ^2	Anisotropy (r)	η_m (mPa s)
13.0	0.1	3.28 7.82	0.16 0.84	1.15	0.122	53.1
13.0	1.5	3.35 8.14	0.18 0.82	1.20	0.142	70.2
13.0	12.0	3.30 7.22	0.25 0.75	1.20	0.105	39.4
2.0	0.2	2.96 8.24	0.14 0.86	1.18	0.27	323.0

plot shows only one inflection corresponding to a CAC value of ca. 0.08 mM. This might be due to closeness of the two CAC values. It should be noted that, in the case of cationic specie, the *r*-value is much higher than that of the anionic form indicating tighter packing of the hydrocarbon chains as compared to the anionic form. Interestingly, for the anionic form, the increase of [C_{12}HHis] beyond the CAC_2 value results in a decrease of the *r*-value which reaches minimum at 12 mM. The *r*-value at this concentration, however, is much smaller and close to that normally observed for small micelles of ionic surfactants. The sigmoid change of *r*-value with concentration is indicative of a phase change and the large bilayer aggregates are transformed into micelles. Perhaps the same may be true with the cationic specie and the large aggregates that are formed from the bilayer aggregates appeared in the form of precipitate. The concentration-dependent phase change of vesicles to micelles has been observed with other N-acyl amino acid surfactants (Khatua and Dey, 2007).

In aid to the above conclusion, we have measured microviscosity (η_m) of the aggregates formed in different concentration ranges. The η_m values were calculated from the steady-state *r*-value and fluorescence lifetime (τ_f) of DPH probe at concentrations corresponding to the maximum and plateau region following a procedure already described in the literature (Roy et al., 2005). The data are collected in Table 2. It is observed that the η_m value for both species at 0.1 mM C_{12}HHis is higher than that of SDS micelles (16.33 mPa s) (Roy et al., 2005) and is consistent with the bilayer structure formation. At [C_{12}HHis] equal to 1.5 mM, η_m for the anionic specie has the highest value. However, the η_m value decreased in the presence of 12 mM C_{12}HHis, but it is higher than that of SDS micelles. This is consistent with the results shown by the plots in Fig. 2. Thus, it can be concluded that initially formed bilayer aggregates are first transformed into another type of bilayer structures, which again are converted to small micelles.

3.3. Transmission electron microscopy (TEM)

To investigate the shape of the microstructures formed by the amphiphile, TEM images (Fig. 5) were taken in aqueous buffer solutions of C_{12}HHis. The micrograph **A** for the acidic solution (0.2 mM, pH 2) in Fig. 5 clearly reveals existence of unilamellar vesicles with internal diameters in the range 50–100 nm. The micrograph **B** of 0.2 mM C_{12}HHis solution at pH 13 also exhibits vesicular structures with internal diameter in the range 20–100 nm. Although it is not very clear, the vesicles look like unilamellar ones. It is interesting to see that the micrograph **C** for1.5 mM solution at pH 13 reveals tubular structures. The tubules are 0.5–2 μm long with inner diameter in the range of 50–70 nm. The tubules might have formed by the fusion of the vesicles that are produced in dilute solution. This is consistent with the results obtained from fluorescence probe studies. However, we were unable to get any good micrograph for the 12 mM solution at pH 13. This is possibly due to smaller size of the micellar aggregates as suggested by the fluorescence probe studies. The branching nanotube formation in pH 13 solution of a structurally similar C_{12}HVal amphiphile has been reported earlier by us (Ghosh and Dey, 2008a). Branching tubular structures in aqueous dispersions of peptide surfactants were also found Zhang and coworkers (Sylvain et al., 2002). On the other hand, Ghadiri and coworkers (Bong et al., 2001; Fernandez-Lopez et al., 2001) have reported that alternating D,L-α-peptides and cyclic β-peptides form self-assembling nanotubes. Tube-like structures were also observed with mixtures of cationic bolaamphiphile and anionic sodium dodecyl surfate (SDS) (Yan et al., 2003; Han et al., 2004; Lu et al., 2006). Lu and coworkers have suggested salt-induced transformation of vesicles to tubules in a catanionic system consisting of a cationic bolaamphiphile and anionic SDS surfactant (Lu et al., 2006).

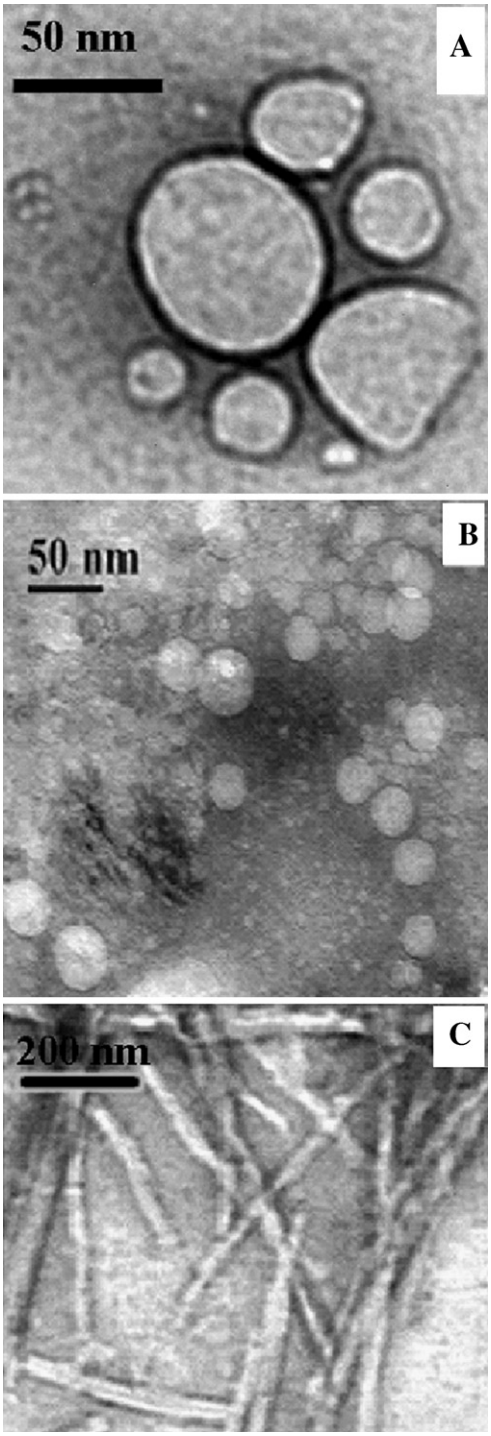

Fig. 5. TEM micrographs of C_{12}HHis in 20 mM phosphate buffer (A) 0.2 mM (pH 2.0) (stained with 0.75% (w/v) uranyl acetate), (B) 0.2 mM (pH 13) and (C) 1.5 mM (pH 13.0) (stained with 0.75% w/v sodium phosphotungstate, pH 13).

3.4. Hydrodynamic size of the aggregates

The mean hydrodynamic diameters of the aggregates formed at different concentrations and pH were also determined by dynamic light scattering (DLS) measurements. The mean hydrodynamic diameters (d_H) of the vesicles formed in pH 2 and 13 solutions of C_{12}HHis are listed in Table 1. The size distributions have been depicted in Fig. 6 (panel (A)). It can be observed that the size of the vesicles formed by C_{12}HHis amphiphile in both acidic and basic pH solutions is very similar to that observed in the respec-

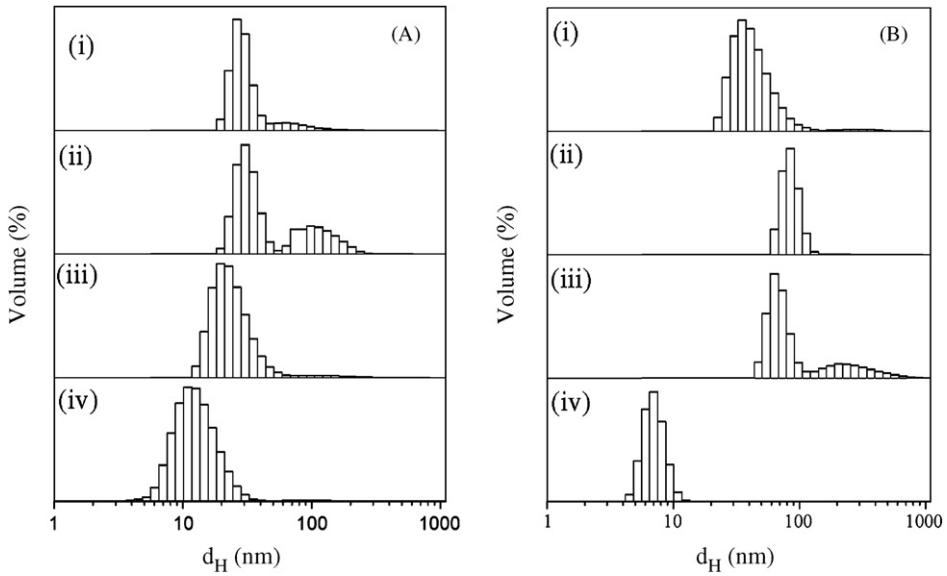

Fig. 6. Panel (A) Size distributions of the aggregates in 20 mM phosphate buffer in pH 2.0: (i) 0.2 mM; in pH 13.0: (ii) 0.2 mM, (iii) 1.5 mM, and (iv) 12.0 mM C_{12}HHis; Panel (B) Size distributions of the aggregates in 20 mM phosphate buffer in pH 2.0: (i) 0.2 mM C_{12}HHis; in pH 13.0: (ii) 0.2 mM, (iii) 1.5 mM, and (iv) 12.0 mM C_{12}HHis in the presence of 10 mol% Chol.

tive TEM picture. The solution at pH 13 containing 1.5 mM C_{12}HHis exhibits bimodal size distributions indicating existence of two different types of aggregates. The smaller particles with higher volume percentage are clearly due to the vesicles. The large particles with smaller volume percentage can be associated to the tubular structures. However, as far as DLS measurement is concerned, they cannot be assigned to any hydrodynamic size because the method is not applicable for nonspherical aggregates. This means that both vesicles and tubular structures are in equilibrium. It is important to observe that the large aggregates disappear and aggregates of much smaller diameters are formed when surfactant concentration is 12 mM. The size of the aggregates is, however, greater than normal spherical micelles and thus can be attributed to ellipsoid or rod-like micelles. This is consistent with the lower microviscosity value (Table 2) obtained from fluorescence anisotropy measurements in 12 mM solution of pH 13. Transition of nanotube to micelles in aqueous solution of potassium N-Acyl phenylalaninate has also been reported recently (Ohta et al., 2006).

3.5. Stability of vesicles and tubules

3.5.1. Effect of salt concentration

Biological systems often contain a large amount of salt (equivalent to 150 mM NaCl). Under this condition the vesicle structures may become unstable thus causing burst release of its content. In fact, such behavior was recently observed by us with an amphiphile sodium 4-(N-octyloxybenzoyl)-L-valinate surfactant (Mohanty et al., 2007). We observed vesicles-to-micelle transition in the presence of salts. The influence of salt concentration on the stability of vesicle formed by C_{12}HHis was investigated by monitoring fluorescence anisotropy (r) of DPH probe in surfactant solutions. Fig. 7 shows the plots of variation of r as a function of [NaCl] for a given concentration of C_{12}HHis at two different pH. It is observed that for both pH 13.0 and 2.0, the r-value does not change significantly with the increase of salt concentration, suggesting no change of shape and size of the vesicles. Indeed, DLS measurements showed no significant change in hydrodynamic diameter in the presence of 200 mM NaCl. This means that the vesicles are quite stable under physiological condition.

3.5.2. Effect of cholesterol

Cholesterol (Chol) is known to increase rigidity and hence stability of the bilayer membrane of liposomes (Roy et al., 2006). In order to increase vesicle stability, we investigated the effect of addition of Chol on the r-value of DPH probe. The results are presented in Fig. 8. It is observed that for the vesicle solutions at pH 2 and 13, the r-value of DPH probe increases with [Chol] reaching maximum at ca. 10% (mol/mol) of Chol. However, the plot for the solution containing tubular aggregates exhibits only a small increase of the r-value in the presence of Chol. DLS measurements, on the other hand, show that hydrodynamic size of the vesicles increases in the presence of 10 mol% Chol at both pH (Table 1). The corresponding size distributions in the presence of 10 mol% Chol for the vesicular and tubular phases have been depicted in panel (B) Fig. 6. It can be observed that the size distribution for the tubular phase also shifts toward larger diameter range. However, it is interesting to note that size of the rod-like micelles in 10 mM C_{12}HHis solution decreased slightly upon addition of Chol. Thus it can be concluded that addition of Chol results in a growth of vesicles as well as tubular aggregates, indicating increase of stability.

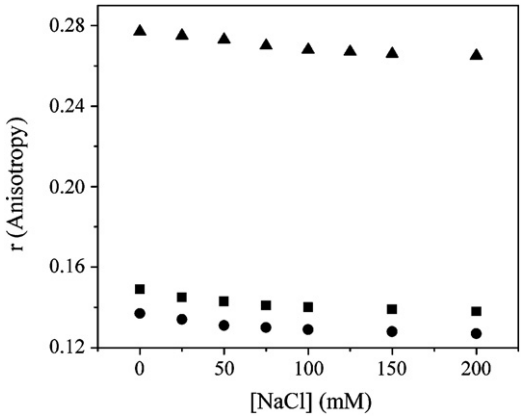

Fig. 7. Variation of fluorescence anisotropy (r) of DPH with [NaCl]: (▲) 0.3 mM C_{12}HHis at pH 2, (■) 0.2 mM C_{12}HHis at pH 13, and (■) 1.0 mM C_{12}HHis at pH 13.

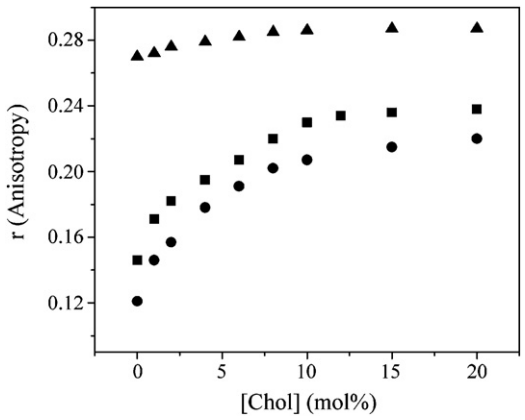

Fig. 8. Variation fluorescence anisotropy (r) of DPH with [Chol] in (▲) 0.3 mM C_{12}HHis at pH 2, (●) 0.2 mM C_{12}HHis at pH 13, (■) 1.0 mM C_{12}HHis at pH 13.

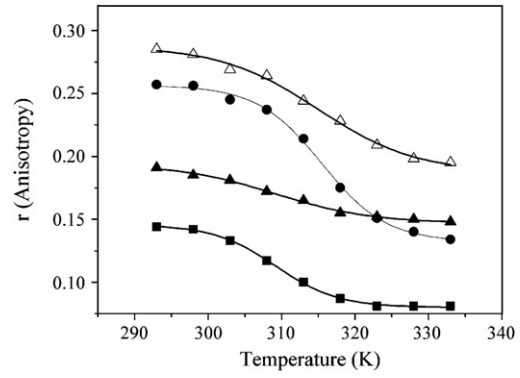

Fig. 9. Plots of fluorescence anisotropy (r) of DPH in 20 mM phosphate buffer versus temperature: (■) 0.1 mM C_{12}HHis, pH 13.0, (▲) 0.1 mM C_{12}HHis containing 10% (mol/mol) cholesterol, pH 13, (●) 0.1 mM C_{12}HHis, pH 2.0, and (△) 0.1 mM C_{12}HHis containing 10% (mol/mol) cholesterol, pH 2.0.

3.5.3. *Effect of temperature*

The temperature stability of the vesicles formed in dilute solution of C_{12}HHis was also investigated by monitoring the steady-state fluorescence anisotropy of DPH probe. The plots in Fig. 9 show the variation of r-value of the DPH probe with temperature. The data were fit to sigmoid curve corresponding to a two-state process. It can be seen that the r-value decreases rapidly with the rise of temperature. This could be attributed to transformation of vesicle to micelles. The vesicle-to-micelle phase transition temperature (T_m) is around 310 K, which is equal to the physiological temperature and thus will have limited use. However, as discussed above, the vesicle stability increased upon addition of Chol. Therefore, we measured the temperature stability of the vesicle phase in the presence of 10% Chol. The plots presented in Fig. 9 show that in the presence of Chol, the r-value decreases only slightly with the rise of temperature, thus broadening the phase transition temperature range. The small change in r-value might be due to increase of chain mobility of the hydrocarbon tail of the amphiphile. The melting temperature is thus enhanced up to 333 K in the presence of 10 mol% Chol, showing enhanced vesicle stability.

4. Conclusions

In summary, the zwitterionic amphiphile C_{12}HHis with L-histidine head group exists in the cationic and anionic forms in phosphate buffers of pH 2 and 13, respectively. The anionic form of the amphiphile is more surface active than the cationic form. The surface tension plots of both forms exhibit two breakpoints corresponding to two CAC values. In dilute solution, both forms of the amphiphile produce unilamellar vesicles with sizes in the nanometer range. In alkaline medium, the vesicles are transformed into nanotubes upon increase of surfactant concentration. The nanotubes are further converted to rod-like micelles at a much higher surfactant concentration. Addition of salt, however, does not affect the stability of the vesicle phase significantly. However, addition of cholesterol increases the stability and size of the vesicles and tubules in solution. The vesicles, in dilute solution, undergo transition to form micelles above a temperature of ca. 310 K. However, vesicle-to-micelle phase transition becomes broad in the presence of 10 mol% cholesterol.

Acknowledgements

This work was supported by grant (No. SR/S1/PC-18/2005) from Department of Science and Technology, New Delhi, India. The authors are thankful to Dr. N. Chattopadhyay, Jadavpur University, Kolkata for his assistance with the fluorescence lifetime measurements. The authors also thank Dr. Nilmoni Sarkar, Department of Chemistry, IIT, Kharagpur for the DLS measurements.

References

Abel, E., De Wall, S.L., De Edwards, W.B., Lalitha, S., Couvey, D.F., Gokel, G.W., 2000. Formation of stable vesicles from *N*- or 3-alkylindoles: possible evidence for tryptophan as a membrane anchor in proteins. J. Org. Chem. 65, 5901–5909.

Bertini, I., Scozzafava, A., 1981. In: Sigel, H. (Ed.), Metal Ions in Biological Systems, vol. 12. Marcel Dekker, New York, pp. 31–74.

Bong, D.T., Clark, T.D., Granja, J.R., Ghadiri, M.R., 2001. Self-assembling organic nanotubes. Angew. Chem. Int. Ed. Engl. 40, 988–1011.

Bonomo, R., Conte, E., Impellizzeri, G., Pappalardo, G., Purrello, R., Rizzarelli, E., 1996. Copper(II) complexes with cyclo(L-aspartyl-L-aspartyl) and cyclo(L-glutamyl-L-glutamyl) derivatives and their antioxidant properties. J. Chem. Soc. Dalton Trans., 3093–3099.

Casolaro, M., Chelli, M., Ginanneschi, M., Laschi, F., Messori, L., Muniz-Miranda, M., Papini, A.M., Kowalik-Jankowska, T., Kozlowsky, H., 2002. Spectroscopic and potentiometric study of the SOD mimic system copper(II)/acetyl-L-histidylglycyl-L-histidylglycine. J. Inorg. Biochem. 89, 181–190.

Félix, M., Goñi, A.A., 2000. Spectroscopic techniques in the study of membrane solubilization, reconstitution and permeabilization by detergents. Biochim. Biophys. Acta 1508, 51–68.

Fernandez-Lopez, S., Kim, H.S., Choi, E.C., Delgado, M., Granja, J.R., Khasanov, A., Kraehenbuehl, K., Long, G., Weinberger, D.A., Wilcoxen, K.M., Gghadiri, M.R., 2001. Antibacterial agents based on the cyclic D,L-α-peptide architecture. Nature (Lond.) 41, 452–455.

Ghosh, A., Dey, J., 2008a. Physicochemical characterization and tube-like structure formation of a novel amino acid-based zwitterionic amphiphile N-(2-hydroxydodecyl)-L-valine in water. J. Phys. Chem. B 112, 6629–6635.

Ghosh, A., Dey, J., 2008b. Effect of hydrogen bonding on the physicochemical properties and bilayer self-assembly formation of N-(2-hydroxydodecyl)-L-alanine in aqueous solution. Langmuir 24, 6018–6026.

Han, F., He, X., Huang, J., Li, Z., Wang, Y., Fu, H., 2004. Surface properties and aggregates in the mixed systems of bolaamphiphiles and their oppositely charged conventional surfactants. J. Phys. Chem. B. 108, 5256–5262.

Hidaka, H., Murata, M., Onai, T., 1984. Helical aggregates of chiral N-(2-hydroxydodecyl) amino acids. Chem. Commun., 562–564.

Huang, J.-B., Mao, M., Zhu, B.-Y., 1999. The surface physico-chemical properties of surfactants in ethanol–water mixtures. Colloids Surf. A 155, 339–345.

Ihara, Y., Hosako, R., Nango, M., Kurok, N., 1981. Efficient synthesis of estriol 16-glucuronide via 2,4,16 α-tribromoestrone. Chem. Commun., 383–384.

Israelachvili, J.N., 1985. Intermolecular and Surface Forces. Academic Press, London.

Khatua, D., Dey, J., 2007. Fluorescence, circular dichroism, light scattering, and microscopic characterization of vesicles of the sodium salts of three N-acyl peptides. J. Phys. Chem. B 111, 124–127.

Kowalik-Jankowska, T., Jasionowski, M., Lankiewicz, L., 1999. Copper(II) complexation by pituitary adenylate cyclase activating polypeptide fragments. J. Inorg. Biochem. 76, 63–70.

Kumar, V.V., Pichon, C., Refregiers, M., Guerin, B., Midoux, P., Chaudhuri, A., 2003. Single histidine residue in head-group region is sufficient to impart remarkable gene transfection properties to cationic lipids: evidence for histidine-mediated membrane fusion at acidic pH. Gene Therapy 10, 1206–1215.

Lu, T., Han, F., Li, Z., Huang, J., Fu, H., 2006. Transitions of organized assemblies in mixed systems of cationic bolaamphiphile and anionic conventional surfactants. Langmuir 22, 2045–2049.

Mohanty, A., Patra, T., Dey, J., 2007. Salt-induced vesicle to micelle transition in aqueous solution of sodium N-(4-octyloxybenzoyl)-L-valinate. J. Phys. Chem. B 111, 7155–7159.

Murase, H., Nagao, A., Terao, J., 1993. Antioxidant and emulsifying activity of N-(long-chain-acyl)histidine and N-(long-chain-acyl)carnosine. J. Agric. Food Chem. 41, 1601–1604.
Nayak, R.R., Roy, S., Dey, J., 2006. Characterization of polymeric vesicles of poly(sodium 11-acrylamidoundecanoate) in water. Colloid Polym. Sci. 285, 219–224.
Nemkovich, N.A., Baumann, W., Kruchenok, Y.V., Reis, H., Rubinov, A.N., 1997. Dipole moments of phenylnaphthylamine fluorescence probes and study of dielectric interactions in human erythrocyte ghosts. J. Fluoresc. 7, 363–370.
Ohkubo, K., Sugahara, K., Ohta, H., Tokuda, K., Ueoka, R., 1981. The stereoselective deacylation of long-chain amino acid esters by comicelles of N-acyl-L-histidine and various cationic surfactants. Bull. Chem. Soc. Jpn. 54, 576–580.
Ohta, A., Danev, R., Nagayama, K., Mita, T., Asakwa, T., Miyagishi, S., 2006. Transition from nanotubes to micelles with increasing concentration in dilute aqueous solution of potassium N-acyl phenylalaninate. Langmuir 22, 8472–8477.
Ragunath, K.G., Bhattacharya, S., 1995. Formation of gel and fibrous microstructures by 1-alkyne amphiphiles bearing L-serine headgroup in organic solvents. Chem. Phys. Lipids 77, 13–23.
Rosen, M.J., 2004. Surfactants and Interfacial Phenomena, 4th ed. Wiley-Interscience, New York.
Roy, S., Mohanty, A., Dey, J., 2005. Microviscosity of bilayer membranes of some N-acyl amino acid surfactants determined by fluorescence probe method. Chem. Phys. Lett. 414, 23–27.
Roy, S., Nayak, R.R., Dey, J., 2006. Stable vesicle formation through intra- and inter-chain aggregation of poly[sodium N-(11-acryl-amidoundecanoyl)-L-valinate] in aqueous solution. Colloids Surf. A: Physicochem. Eng. Aspects 290, 62–69.
Saitoh, T., Matsushima, S., Hiraide, M., 2007. Flotation of polycyclic aromatic hydrocarbons coprecipitated with aluminum hydroxide containing sodium dodecyl sulfate and magnesium. Colloids Surf. A: Physicochem. Eng. Aspects 299, 88–92.
Shinitzky, M., 1984. Physical Methods on Biological Membranes and their Model Systems. Plenum Publishing Corp., New York, 237 pp.
Smith, G.D., Barden, R.E., 1975. Some physico-chemical properties of aqueous solutions of N^{α}-acyl-L-histidine. Chem. Phys. Lipids 14, 1–14.
Sylvain, V., Santoso, S., Gong, H., Watson, N., Zhang, S., 2002. Molecular self-assembly of surfactant-like peptides to form nanotubes and nanovesicles. Proc. Natl. Acad. Sci. U.S.A. 99, 5355–5360.
Velázquez, M.M., Ortega, F., Monroy, F., Rubio, R.G., Pegiadou, S., Pérez, L., Infante, M.R., 2005. Langmuir monolayers of zwitterionic surfactant hexadecyl 1-N-L-tryptophan glycerol ether. J. Colloid Interface Sci. 283, 144–152.
Wang, L., Jacobi, S., Sun, J., Overs, M., Fuchs, H., Schaefer, H.J., Zhang, X., Shen, J., Chi, L., 2005. Anisotropic aggregation and phase transition in Langmuir monolayers of methyl/ethyl esters of 2,3-dihydroxy fatty acids. J. Colloid Interface Sci. 285, 814–820.
Watanabe, N., Nakajima, T., Touhara, H., 1988. Graphite Fluorides. Elsevier, Amsterdam.
Yan, Y., Huang, J., Li, Z., Han, F., Ma, J., 2003. Aggregates transition depending on the concentration in the cationic bolaamphiphile/SDS mixed systems. Langmuir 19, 972–974.
Zana, R., In, M., Lévy, H., 1997. Alkanediyl-α,ω-bis(dimethylalkylammonium bromide). 7. Fluorescence probing studies of micelle micropolarity and microviscosity. Langmuir 13, 5552–5557.